

# High-Resolution Structure of the Eukaryotic 80S Ribosome

Gulnara Yusupova and Marat Yusupov

Institut de Génétique et de Biologie Moléculaire et Cellulaire, Université de Strasbourg, Strasbourg F-67000, France

INSERM and CNRS, UMR7104, Illkirch F-67400, France; email: gula@igbmc.fr, marat@igbmc.fr

Annu. Rev. Biochem. 2014. 83:467–86

First published online as a Review in Advance on February 21, 2014

The *Annual Review of Biochemistry* is online at [biochem.annualreviews.org](http://biochem.annualreviews.org)

This article's doi:  
10.1146/annurev-biochem-060713-035445

Copyright © 2014 by Annual Reviews.  
All rights reserved

## Keywords

yeast, crystallography, core, protein, RNA, expansion segment

## Abstract

The high-resolution structure of the eukaryotic ribosome from yeast, determined at 3.0-Å resolution, permitted the unambiguous determination of the protein side chains, eukaryote-specific proteins, protein insertions, and ribosomal RNA expansion segments of the 80 proteins and ~5,500 RNA bases that constitute the 80S ribosome. A comparison between this first atomic model of the entire 80S eukaryotic ribosome and previously determined structures of bacterial ribosomes confirmed early genetic and structural data indicating that they share an evolutionarily conserved core of ribosomal RNA and proteins. It also confirmed the conserved organization of essential functional sites, such as the peptidyl transferase center and the decoding site. New structural information about eukaryote-specific elements, such as expansion segments and new ribosomal proteins, forms the structural framework for the design and analysis of experiments that will explore the eukaryotic translational apparatus and the evolutionary forces that shaped it. New nomenclature for ribosomal proteins, based on the names of protein families, has been proposed.

## Contents

|  |     |
|--|-----|
| INTRODUCTION .....                                 | 468 |
| Background .....                                   | 468 |
| Isolation of Ribosomes for X-Ray<br>Analysis ..... | 469 |
| Structure Determination .....                      | 470 |
| THE ARCHITECTURE OF THE<br>80S YEAST RIBOSOME..... | 471 |
| Core of the Ribosome.....                          | 471 |
| New Nomenclature of Ribosomal<br>Proteins .....    | 474 |
| Expansion Segments .....                           | 474 |
| Intersubunit Bridges .....                         | 474 |
| Peptide Exit Tunnel .....                          | 480 |
| PERSPECTIVES OF YEAST<br>RIBOSOME                  |     |
| CRYSTALLOGRAPHY.....                               | 480 |
| Nonribosomal Protein Stm1.....                     | 480 |
| Translocation and Domain<br>Motions .....          | 482 |

## INTRODUCTION

### Background

It has long been recognized that a complete understanding of the mechanism of translation ultimately depends on determining the molecular structure of the ribosome, the largest and most complicated RNA–protein assembly in the cell, that translates the genetic code into proteins. A ribosome from bacteria and archaea consists of a large (50S) subunit and a small (30S) subunit, which together constitute the 2.5-megadalton (MDa) 70S ribosome. Their eukaryotic counterparts are the 60S and 40S subunits and the 80S ribosome (from 3.5 MDa in lower eukaryotes to 4.5 MDa in higher eukaryotes). Many key ribosomal components are conserved across the three domains of life—bacteria, archaea, and eukarya—and constitute a common core that performs the fundamental processes of protein biosynthesis (for a review, see Reference 1). The process of protein synthesis has been studied during the past 50 years, but until recently, detailed information about

the three-dimensional structure of the ribosome had been unavailable. Recent years have seen many exciting advances in structure determination of prokaryotic ribosome particles and the entire prokaryotic ribosome, vacant or complexed with its functional ligands; these advances were enabled by the use of X-ray crystallography and cryo–electron microscopy (cryo-EM). Cryo-EM and single-particle analyses enabled the first direct visualizations of the bacterial ribosome in different functional states (2–5). However, not until the determination of X-ray crystallographic structures of the entire prokaryotic 70S ribosome, as well as of the individual prokaryotic 30S and 50S subunits, did accurate atomic models become available (6–12).

That X-ray crystallography can provide high-resolution structures of macromolecules such as the ribosome has been known for decades, but for such structures to be obtained the macromolecule must be crystallized. Thus, for many years there were no ribosome crystals. Initial progress in the method development of crystallization of the 50S ribosomal subunits isolated from *Bacillus stearothermophilus* and *Haloarcula marismortui* (13–15), as well as of the 30S subunit and full 70S ribosome isolated from *Thermus thermophilus* (16–20), enabled advances in ribosome crystallography. The introduction and development of innovative methodologies, such as improvements in synchrotron sources, computing, X-ray detectors, and crystallographic software, have also been essential.

During the past 10 years, investigators have also made remarkable progress in full prokaryotic 70S ribosome crystallography, and one can now obtain, at medium or high resolution, not only the structure of the vacant ribosome but also the structure of the 70S ribosome with key components bound. These structural studies of the prokaryotic 70S ribosome functional complexes span several steps in protein elongation and termination and are reviewed elsewhere (21–23).

However, until recently, our knowledge about the structural organization of the eukaryotic ribosome was based only on fitting

high-resolution crystal structures of prokaryotic ribosomes into medium-resolution cryo-EM single-particle reconstructions (24–26). Cryo-EM studies provided the first models of the eukaryotic ribosome at 6–15-Å resolution, as well as a much broader spectrum of prokaryotic and eukaryotic ribosome complexes for investigating the mechanisms of translocation (27–29) and protein transport (26, 30).

Despite this progress, we could not discern the relationship between the structure and function of the eukaryotic ribosome at the atomic level. As mentioned above, at present only X-ray crystallography can provide high-resolution structures of the eukaryotic ribosome; until 2010, no three-dimensional crystals of the eukaryotic ribosome or ribosome particles had been reported. The eukaryotic 80S ribosome has an ~40% larger mass than its prokaryotic counterpart, and this high complexity was the main obstacle to obtaining well-diffracting crystals suitable for X-ray crystallography. Our previous experience in obtaining the first crystals of the entire prokaryotic 70S ribosome and its structural determination (6, 12, 16–20) was a useful background for developing new approaches that allowed us to create diffracting crystals of the eukaryotic full 80S ribosome from *Saccharomyces cerevisiae*. Crystal structures of this ribosome from *S. cerevisiae*, with a mass of ~3.3 MDa, were determined first at 4.2-Å and later at 3.0-Å resolution. These structures have significantly advanced the field in investigating protein synthesis and its regulation in the cell (31, 32). The ciliate protozoa *Tetrahymena thermophila* was recently used for crystallization. The structures of the 40S and 60S ribosomal subunits from *T. thermophila* were determined at 3.9-Å and 3.5-Å resolution, respectively, and provided information about their interaction with the initiation factors eIF1 and eIF6 (33–35).

This review summarizes recent studies of the eukaryotic full 80S ribosome structure performed by X-ray crystallography. We focus on recent work from our laboratory.

## Isolation of Ribosomes for X-Ray Analysis

The main challenge in crystallographic studies of the ribosome is finding well-diffracting crystals. Ensuring that the isolated samples of the ribosome are highly homogeneous and can form well-ordered crystals is very important. This step differs from cryo-EM sample preparation, wherein investigators select particles of similar conformation for structure determination (36).

We developed new methods of ribosome purification to crystallize prokaryotic and eukaryotic ribosomes. For the prokaryotic studies, we used an extreme-thermophilic bacterium, *Thermus thermophilus*. In the early 1980s, we introduced this extreme thermophile to the field of ribosomal crystallography because the ribosomes isolated from this organism are robust and resistant to degradation (16, 17, 37). Obtaining the entire 70S ribosome in its monosome form was a difficulty we faced in developing new protocols, given that a significant fraction of 70S ribosomes in cell extracts are in the form of polysomes. A traditional way to isolate monoribosomes from polysomes in bacteria is based on salt washing in 0.5 to 1.0 M of  $\text{NH}_4\text{Cl}$ ,  $\text{KCl}$ , or  $\text{CsCl}_2$ , which removes ligands from the ribosomes. We developed a purification protocol for *T. thermophilus* 70S ribosomes that includes this harsh salt treatment at the first stage of purification. To improve the quality of the ribosome, we introduced an additional treatment step that involves binding ribosomes to a chromatographic resin (butyl-TOYOPEARL<sup>®</sup> hydrophobic resin) (6, 37, 38). We optimized the ionic conditions used for chromatography to obtain 70S ribosomal tight couples. As a result, we obtained crystals of *T. thermophilus* 70S ribosomes from the samples purified without dissociation of the 70S ribosome into the ribosomal subunits (6, 12, 17, 38). This approach to ribosome purification with hydrophobic chromatography was subsequently used to optimize crystallization and solve the structures of the *T. thermophilus* small (30S) ribosome particle (10, 39) and the 70S ribosome (12, 40).

We optimized various ribosome-purification procedures to develop a suitable isolation protocol for yeast ribosomes. Conventional ways to isolate eukaryotic monoribosomes from polysomes by salt washing produce 80S ribosomes that fail to crystallize. On the basis of previous experiences with other fragile systems (41), we established a radically new approach employing very mild manipulations. This gentle isolation protocol ensures that the ribosomes are in monosome form and that all ribosome components are intact and present. To achieve these goals, we exploited the observation that glucose starvation (42) of growing yeast cells inhibits initiation and causes accumulation of very homogeneous ribosomes without any ligands, thereby obviating the requirement for harsh salt-washing steps. We accomplished gentle cell lysis by shaking the cells with glass beads, followed by polyethylene glycol fractionation of cell extracts and sedimentation of ribosomes through a sucrose gradient (31, 32).

## Structure Determination

The initial crystals diffracted poorly but were improved by soaking with various dehydration agents and metal ions. These improvements yielded three crystal forms: type I with four ribosomes in the asymmetric unit and types II and III with two. All three types belonged to space group  $P2_1$ , but their cell parameters differed. Type III crystals diffracted to a resolution higher than 3 Å. Molecular replacement procedures found clear solutions in all the crystal forms by use of a search model composed of the large subunit (50S) from *H. marismortui* (11) and the small subunit (30S) from *T. thermophilus* (43). This solution, following phase improvement through rigid-body refinement, was used to locate several hundred osmium sites in type III crystals and thus obtain initial single-anomalous dispersion (SAD) phases. We performed the following steps: (a) phase improvement using solvent flattening and intercrystal and noncrystallographic averaging between the three forms; (b) expansion of the model by manual building, followed by

rigid-body refinement of large domains; and (c) location of additional osmium sites by use of the expanded model and map recalculation. When the model approached completion, the number of located osmium sites reached 700.

The model consisted of two ribosomes in the asymmetric unit of type III crystals and contained the entire ribosomal RNA (rRNA) moiety, except for a single flexible expansion segment (ES), ES27, and a small part of ES7, both in the 60S subunit. The density of the phosphates was usually unambiguous and guided modeling of the rRNA parts. The model also contained the C $\alpha$  backbone of all proteins with homologs in prokaryotic ribosome X-ray structures, including, in most cases, their eukaryote-specific additions. This structure was determined at 4.2-Å resolution (32).

To extend the resolution of the electron-density maps, we collected data from 13 isomorphous crystals (31). Improvements in crystal treatment and data-collection methodology were also instrumental in obtaining a full data set at 3.0-Å resolution (31). We combined the phases obtained from the refined lower-resolution model with experimental SAD phases derived from ~1,400 osmium hexamine sites. The last round of model refinement was  $R_{\text{free}}/R_{\text{work}} = 22.8\%/18.2\%$ . The final model consisted of two ribosomes in the asymmetric unit, termed ribosomes A and B, that differed markedly in the degree of rotation of the 40S subunit relative to the 60S subunit (4° in ribosome A and 9° in ribosome B) and in the extent of 40S head swiveling (15.5° in ribosome A and 10.5° in ribosome B).

Ordered protein side chains were clearly visible in the electron-density maps, and in most cases, we could distinguish between rRNA purines and pyrimidines. Most yeast ribosomal proteins have duplicate genes (44), and in several cases the high quality of the X-ray data allowed us to determine the differences in the amino acid sequences between isoforms of ribosomal proteins (31).

A mass spectrometry analysis identified Stm1 as the only nonribosomal component of the ribosome preparations, and we traced

residues 21–177 of this protein. The final model contained all 44 proteins that are absent in bacteria and all 35 universally conserved proteins, with the exception of the highly mobile protein L1, regions within the L7/L12 stalk proteins, and residues located in disordered loops or tails. The rRNA was modeled almost completely, except for the major hairpin of ES27L, part of the L1 stalk, and a small part of ES7L. This model included ~90.5% of all ~13,000 ribosomal protein residues and 96.5% of the ~5,500 rRNA residues. Approximately 2,000 metal ions were also present.

## THE ARCHITECTURE OF THE 80S YEAST RIBOSOME

### Core of the Ribosome

Both bacterial 70S and yeast 80S ribosomes are asymmetric assemblies comprising more than 50 different proteins and three or four RNA chains (to see an overall view of prokaryotic and eukaryotic ribosomes, see **Supplemental Video 1**; follow the **Supplemental Material link** in the online version of this article or at <http://www.annualreviews.org>). Each ribosomal component is present in a single copy, except for the stalk proteins L7/L12 and P1/P2, which are present in four or six copies. Early genetic data, corroborated by structural studies, revealed that bacterial and eukaryotic ribosomes share a common structural core, which comprises 34 conserved proteins (15 in the small subunit and 19 in the large subunit) and ~4,400 RNA bases that harbor the major functional centers of the ribosomes, such as the decoding site, the peptidyl transferase center, and the transfer RNA (tRNA)-binding sites (1, 24, 45).

Apart from the core (**Figure 1**), each ribosome contains a unique set of specific moieties: domain-specific proteins, insertions and extensions of conserved proteins, and ESs of rRNAs (46, 47). The 70S ribosome contains 20 bacteria-specific proteins (6 in the 30S subunit and 14 in the 50S subunit); a few extensions of the conserved proteins; such as

proteins S2, S3, and S4; and a few extensions of rRNA, such as helices h6, h17, and h33a in 16S rRNA and helices H1 and H68 in 23S rRNA. The 80S ribosome contains 46 eukaryote-specific proteins (18 in the 40S subunit and 28 in the 60S subunit) and extensions and insertions in most of the proteins of the core, and the rRNA contains several extensions in the conserved rRNA chains; its total length is 900 or more bases. Most of these rRNA and protein moieties envelop the core from the solvent side and therefore are accessible for potential interactions with molecular partners, such as translation factors and chaperones.

The composition of ribosomes may also vary within bacteria, within eukaryotes, and within a single species (although to a lesser extent) under different conditions of growth and stress. Within each domain of life, ribosomes usually contain the same set of rRNA and protein chains, and all divergence is achieved via alterations of the length and sequence of ribosomal components, mainly rRNA. In eukaryotes, the size of the 80S ribosome varies within an ~1-MDa range, mainly owing to insertions in four RNA ESs (ES7L, ES15L, ES27L, and ES39L) in the 25–28S rRNA. In a few cases, ribosomes contain one fewer or one additional ribosomal protein. The 30S and 40S subunits have similar shapes, including the landmarks known as the head, body, platform, beak, and shoulder (**Figure 2a,c**). The messenger RNA (mRNA)- and tRNA-binding sites (A, P, and E) are located on the subunit interface. The mRNA enters through a tunnel located between the head and the shoulder and wraps around the neck of the 30S subunit. The mRNA exit site (the 5' end of the mRNA) is located between the head and the platform (48, 49). The decoding center of the small subunit, where the codon and anticodon are paired and convey fidelity to mRNA decoding, is located on the interface surface and is made of three domains from the head, the shoulder, and the penultimate stem. When one compares the overall structures, it is evident that there is no difference between the decoding centers of eukaryotes and bacteria but that there are

 **Supplemental Material**

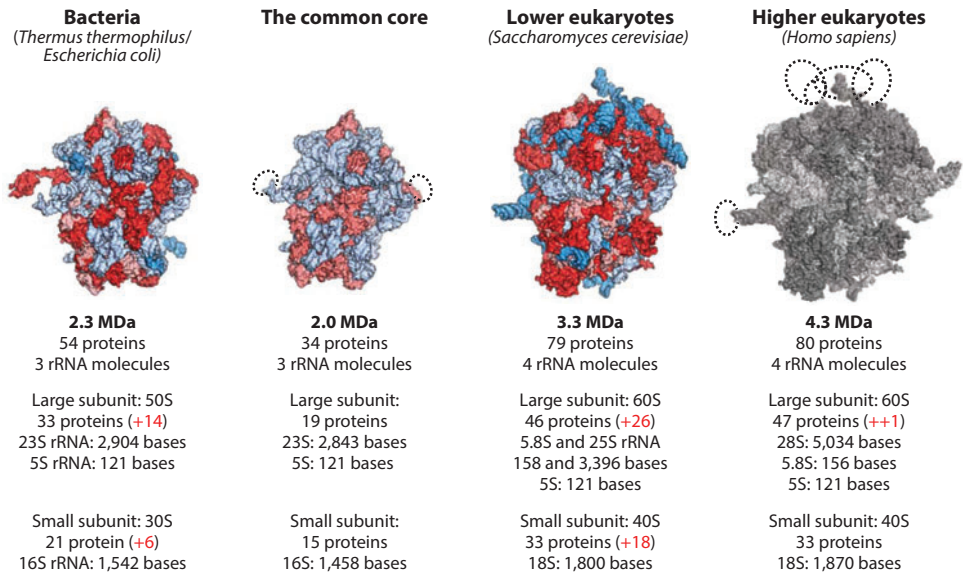


**Figure 1**

Composition of bacterial and eukaryotic ribosomes and the common core. Bacterial and eukaryotic ribosomes share a massive conserved core built of RNA (*light blue*) and proteins (*light red*). Ribosomes in each domain of life contain their own set of proteins in addition to the core: extensions in conserved proteins (*both in red*) and extensions in ribosomal RNA (rRNA) (*blue*). Both 5.8S and 25–28S rRNA molecules are homologous to 23S rRNA in bacteria. Dashed lines around the core indicate positions of flexible stalks that are usually disordered in X-ray structures. For the sake of simplicity, these lines are not shown on other structures. The 80S structure of higher eukaryotes has not been determined by X-ray analysis but is highly similar to the solved structures of yeast and *Tetrahymena thermophila* ribosomes. On the panel of human ribosomes, the yeast 80S structure appears in gray scale, and dashed lines indicate the positions of long RNA expansion segments, the most distinctive characteristic of ribosomes from higher eukaryotes. Based on X-ray and cryo–electron microscopy structures from References 31, 40, 43, 59, and 81–87.

extensive differences between the solvent sides of the small ribosomal subunits.

The 50S and 60S subunits have similar overall crownlike shapes, which encompass the central protuberance, the L1 stalk, and the L7/L12 stalk (in prokaryotes) or the P stalk (in eukaryotes) (**Figure 2b**). On the 60S ribosomal subunit, 27 eukaryote-specific proteins, multiple insertions and extensions of conserved proteins, and several rRNA ESs are concentrated on the periphery of the subunit, forming an almost continuous ring-shaped assembly that envelopes the core (**Figure 1**). This ring-shaped assembly comprises two clusters of eukaryote-specific moieties, about which little is known in terms of biological function.

Located on the interface side of the large ribosomal subunit are the three tRNA-

binding sites (A, P, and E) and the peptidyl transferase center, where the peptide bond formation is catalyzed. This peptidyl transferase center is adjacent to the entrance of a tunnel, along which nascent proteins progress before they emerge from the ribosome on the solvent side. The overall absence of bacteria- and eukaryote-specific moieties on the central regions of both the solvent and interface sides of the subunit is consistent with the universally conserved functions of these areas. The surface of the peptidyl transferase center is also devoid of bacteria- and eukaryote-specific moieties, as is the area around the peptide tunnel on the solvent side, which is used for ribosome association with membranes during protein synthesis (**Figure 2b,d**).

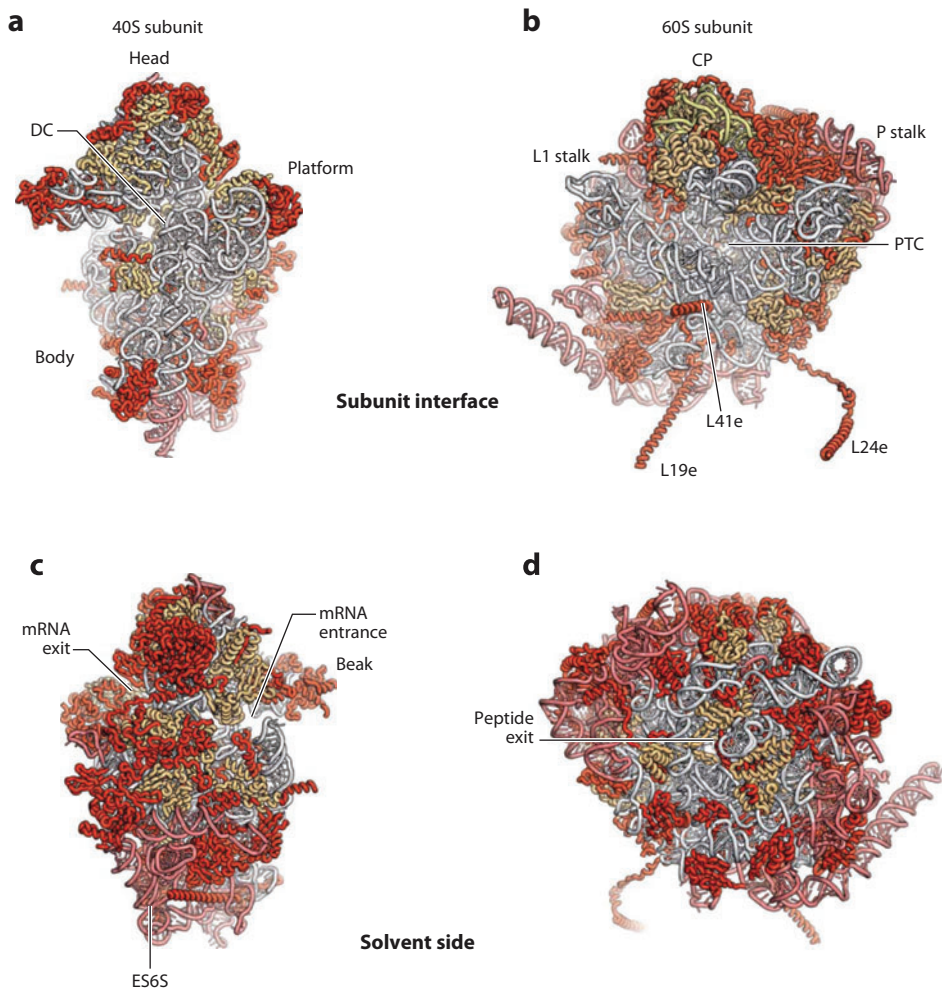


**Figure 2**

View from (a,b) the interface and (c,d) the solvent side of ribosomal subunits of the yeast ribosome, showing the decoding center (DC), head, body, platform, beak, and shoulder in the small subunit and the central protuberance (CP), peptidyl transferase center (PTC), L1 stalk, and P stalk in the large subunit. The common core consists of ribosomal RNA (white) and proteins (light orange); eukaryote-specific moieties are shown in red. Abbreviation: mRNA, messenger RNA.

The high sequence and structural conservation of the decoding and peptidyl transferase centers, as well as of the tRNA substrates, suggests that the knowledge about both the mechanism of decoding genetic information (50, 51) and the peptide-bond formation that we have gained from studies on prokaryotic and archaeal ribosomes can be applied to eukaryotic ribosomes (52). This observation indicates that, in general, the mechanism of elongation in eu-

karyotic protein synthesis is very similar to that in prokaryotes. Also, we expect that eukaryote-specific elements are involved in regulation of initiation, termination, and recycling of translation (53). All these translation steps in eukaryotes are much more complex. For example, eukaryotic initiation requires a multifunctional complex of *trans*-acting factors bound to the ribosome that are as massive as the ribosome itself (54, 55).

## New Nomenclature of Ribosomal Proteins

To facilitate comparison between ribosomes from different species, we adopted a nomenclature system that is based on the names of protein families (<http://www.uniprot.org/docs/ribosomp>) (Table 1). In this convention, the default name for any protein in the universally conserved core (i.e., with bacterial homologs) is the bacterial name because that is the name given to the entire protein family. Eukaryotic proteins lacking bacterial homologs have names that end with the letter e. Exceptions to these rules are as follows: The name *S. cerevisiae* (instead of the protein family name) is used for eukaryote-specific proteins whose protein family names are derived from mammals and have an additional letter A (56). For example, the yeast protein S1, which belongs to the protein family S3Ae, is termed S1e. **Figure 3** shows the positions of all the ribosomal proteins on the surface of the ribosome.

## Expansion Segments

The rRNA expansion elements are located predominantly on the periphery of the solvent-exposed sides of both subunits (**Figure 4a–d**). As mentioned above, the interface between the ribosomal subunits, as well as the area around the mRNA entrance and the polypeptide exit tunnel, is highly conserved and contains very few ESs and eukaryote-specific protein parts (31). The most impressive example of a eukaryotic ES is the ~200-nt-long ES6S in the small ribosomal subunit. This ES emerges at the solvent side of the platform, where it is enveloped by several eukaryote-specific proteins, including a 60-amino-acid-long  $\alpha$ -helical extension of the C terminus of protein L19e (**Figure 4a,b**). ES6S then extends one of its two long arms in the direction of the shoulder, where it interacts with protein S8. The second long arm of this ES runs down toward the bottom of the small subunit. The tip of the second arm is located ~120 Å away from the tip of the first arm. ES6S is in contact with the ribosomal components

that form part of both the exit and entry sites of the mRNA. Therefore, ES6S may be involved in translation initiation, perhaps as a docking surface for factors that participate in activities on both the mRNA exit and entry sites (57).

Unlike prokaryotic rRNA, eukaryotic ESs are rich in irregular nonhelical elements. In two-dimensional diagrams, rRNA is represented by helices connected by irregular linkers, but three-dimensional crystal structures reveal that in prokaryotes these linkers form regular, double-stranded extensions of neighboring helices (10, 11). In contrast, the 80S ribosome structure reveals that long linkers within several ESs of 25S rRNA form nonhelical, mostly single-stranded elements—a unique characteristic of eukaryote-specific rRNA (31). These linkers, which contain high levels of unpaired nucleotides that neither stack with neighboring nucleotides nor participate in any RNA–RNA interactions, play a dominant role in the association between rRNA ESs and proteins. Multiple interactions with several proteins that employ different binding modes can be packed within a short, single-stranded stretch, as exemplified by the shortest stretch in ES39L. The application of such stretches as a platform for protein binding evokes Sm protein assembly onto the single-stranded Sm-site RNA in spliceosome small nuclear ribonucleic particles (58).

## Intersubunit Bridges

Intersubunit bridges are important because they maintain communication pathways between the small and large subunits during protein synthesis. During translation, the ribosome undergoes global conformational rearrangements that are required for mRNA and tRNA translocation, termination, and other processes. These changes involve intersubunit rotation and swiveling of the head domain of the small subunit. The interactions between the ribosomal subunits change with each rearrangement and are dynamic in composition. The 80S ribosome model derived from crystals captured the ribosome in the rotated state.

Several eukaryote-specific bridges were visualized in low-resolution cryo-EM studies of

**Table 1** Nomenclature for ribosomal proteins

|               | Taxonomic range <sup>a</sup> | Bacteria | Yeast | Human |
|---------------|------------------------------|----------|-------|-------|
| Small subunit | B                            | S1       | —     | —     |
| S1e           | A, E                         | —        | S1    | S3A   |
| S2            | B, A, E                      | S2       | S0    | SA    |
| S3            | B, A, E                      | S3       | S3    | S3    |
| S4            | B, A, E                      | S4       | S9    | S9    |
| S4e           | A, E                         | —        | S4    | S4    |
| S5            | B, A, E                      | S5       | S2    | S2    |
|               | B                            | S6       | —     | —     |
| S6e           | A, E                         | —        | S6    | S6    |
| S7            | B, A, E                      | S7       | S5    | S5    |
| S7e           | E                            | —        | S7    | S7    |
| S8            | B, A, E                      | S8       | S22   | S15A  |
| S8e           | A, E                         | —        | S8    | S8    |
| S9            | B, A, E                      | S9       | S16   | S16   |
| S10           | B, A, E                      | S10      | S20   | S20   |
| S10e          | E                            | —        | S10   | S10   |
| S11           | B, A, E                      | S11      | S14   | S14   |
| S12           | B, A, E                      | S12      | S23   | S23   |
| S12e          | E                            | —        | S12   | S12   |
| S13           | B, A, E                      | S13      | S18   | S18   |
| S14           | B, A, E                      | S14      | S29   | S29   |
| S15           | B, A, E                      | S15      | S13   | S13   |
|               | B                            | S16      | —     | —     |
| S17           | B, A, E                      | S17      | S11   | S11   |
| S17e          | A, E                         | —        | S17   | S17   |
|               | B                            | S18      | —     | —     |
| S19           | B, A, E                      | S19      | S15   | S15   |
| S19e          | A, E                         | —        | S19   | S19   |
|               | B                            | S20      | —     | —     |
|               | B                            | S21      | —     | —     |
|               | B                            | THX      | —     | —     |
| S21e          | E                            | —        | S21   | S21   |
| S24e          | A, E                         | —        | S24   | S24   |
| S25e          | A, E                         | —        | S25   | S25   |
| S26e          | E                            | —        | S26   | S26   |
| S27e          | A, E                         | —        | S27   | S27   |
| S28e          | A, E                         | —        | S28   | S28   |
| S30e          | A, E                         | —        | S30   | S30   |
| S31e          | A, E                         | —        | S31   | S27A  |
| RACK1         | E                            | —        | Asc1  | RACK1 |

(Continued)

**Table 1 (Continued)**

|               | Taxonomic range <sup>a</sup> | Bacteria | Yeast | Human |
|---------------|------------------------------|----------|-------|-------|
| Large subunit |                              |          |       |       |
| L1            | B, A, E                      | L1       | L1    | L10A  |
| L2            | B, A, E                      | L2       | L2    | L2    |
| L3            | B, A, E                      | L3       | L3    | L3    |
| L4            | B, A, E                      | L4       | L4    | L4    |
| L5            | B, A, E                      | L5       | L11   | L11   |
| L6            | B, A, E                      | L6       | L9    | L9    |
| L6e           | E                            | —        | L6    | L6    |
| L8e           | A, E                         | —        | L8    | L7A   |
|               | B                            | L9       | —     | —     |
| L11           | B, A, E                      | L11      | L12   | L12   |
|               | B                            | L12/L7   | —     | —     |
| L13           | B, A, E                      | L13      | L16   | L13A  |
| L13e          | A, E                         | —        | L13   | L13   |
| L14           | B, A, E                      | L14      | L23   | L23   |
| L14e          | A, E                         | —        | L14   | L14   |
| L15           | B, A, E                      | L15      | L28   | L27A  |
| L15e          | A, E                         | —        | L15   | L15   |
| L16           | B, A, E                      | L16      | L10   | L10   |
|               | B                            | L17      | —     | —     |
| L18           | B, A, E                      | L18      | L5    | L5    |
| L18e          | A, E                         | —        | L18   | L18   |
|               | B                            | L19      | —     | —     |
| L19e          | A, E                         | —        | L19   | L19   |
|               | B                            | L20      | —     | —     |
| L20e          | E                            | —        | L20   | L18A  |
|               | B                            | L21      | —     | —     |
| L21e          | A, E                         | —        | L21   | L21   |
| L22           | B, A, E                      | L22      | L17   | L17   |
| L22e          | E                            | —        | L22   | L22   |
| L23           | B, A, E                      | L23      | L25   | L23A  |
| L24           | B, A, E                      | L24      | L26   | L26   |
| L24e          | A, E                         | —        | L24   | L24   |
|               | B                            | L25      | —     | —     |
|               | B                            | L27      | —     | —     |
| L27e          | E                            | —        | L27   | L27   |
|               | B                            | L28      | —     | —     |
| L28e          | E                            | —        | —     | L28   |
| L29           | B, A, E                      | L29      | L35   | L35   |
| L29e          | E                            | —        | L29   | L29   |
| L30           | B, A, E                      | L30      | L7    | L7    |
| L30e          | A, E                         | —        | L30   | L30   |
|               | B                            | L31      | —     | —     |

(Continued)

**Table 1** (Continued)

|       | Taxonomic range <sup>a</sup> | Bacteria | Yeast                   | Human   |
|-------|------------------------------|----------|-------------------------|---------|
| L31e  | A, E                         | —        | L31                     | L31     |
|       | B                            | L32      | —                       | —       |
| L32e  | A, E                         | —        | L32                     | L32     |
|       | B                            | L33      | —                       | —       |
| L33e  | A, E                         | —        | L33                     | L35A    |
|       | B                            | L34      | —                       | —       |
| L34e  | A, E                         | —        | L34                     | L34     |
|       | B                            | L35      | —                       | —       |
|       | B                            | L36      | —                       | —       |
| L36e  | E                            | —        | L36                     | L36     |
| L37e  | A, E                         | —        | L37                     | L37     |
| L38e  | A, E                         | —        | L38                     | L38     |
| L39e  | A, E                         | —        | L39                     | L39     |
| L40e  | A, E                         | —        | L40                     | L40     |
| L41e  | A, E                         | —        | L41                     | L41     |
| L43e  | A, E                         | —        | L43                     | L37A    |
| L44e  | A, E                         | —        | L42                     | L36A    |
| P1/P2 | A, E                         | —        | P1/P2 ( $\alpha\beta$ ) | LP1/LP2 |
| P0    | B, A, E                      | L10      | P0                      | LP0     |

<sup>a</sup>Abbreviations: A, archaea; B, bacteria; E, eukarya.

the yeast ribosome (24, 25). Our model, at 3.0-Å resolution, provided an accurate and detailed view of the molecular components involved in these contacts between ribosomal subunits (**Figure 4f**). The evolutionary conservation of intersubunit bridges at the core of the ribosome is noteworthy: Each intersubunit bridge that has been described in the crystal structure of the bacterial ribosome (12) has a corresponding bridge in the eukaryotic ribosome. At the same time, the interaction surface between the two subunits is nearly doubled in eukaryotes due to the appearance of additional bridges (**Figure 4f**). There are seven bridges in the ribosomal core, as well as a few bacteria- and eukaryote-specific bridges (12, 31, 40, 59). In virtually all of the additional bridges, the vast majority of the participating components on both subunits are eukaryote specific. In striking contrast to bacteria, proteins play the dominant role in forming eukaryote-specific bridges (12), which are located on the periphery of the subunit interface and on the solvent sides of both

subunits. The appearance of these numerous additional bridges on the outer edge of the eukaryotic subunit interface, which significantly increases the interaction surface between subunits, may be the reason for the preferential rotated state of eukaryotic ribosomes (31, 60, 61).

Only one eukaryote-specific bridge is positioned at the center of the ribosome: bridge eB14 (**Figure 4f**). This bridge is formed by protein L41e, the smallest protein in yeast cells (25 amino acids), which consists of a single  $\alpha$ -helix that is enveloped by conserved core rRNA (**Figure 2b**). Protein L41e protrudes from the 60S subunit into the 40S subunit in the proximity of the decoding center and is nearly buried in a binding pocket composed of helices h27, h45, and h44. This bridge has two remarkable characteristics. First, the binding pocket of protein L41e in the small subunit is highly conserved in eukaryotes and bacteria. Second, in the context of the full ribosome, protein L41e is much more strongly associated with the 40S subunit than with the 60S subunit. Interestingly, although



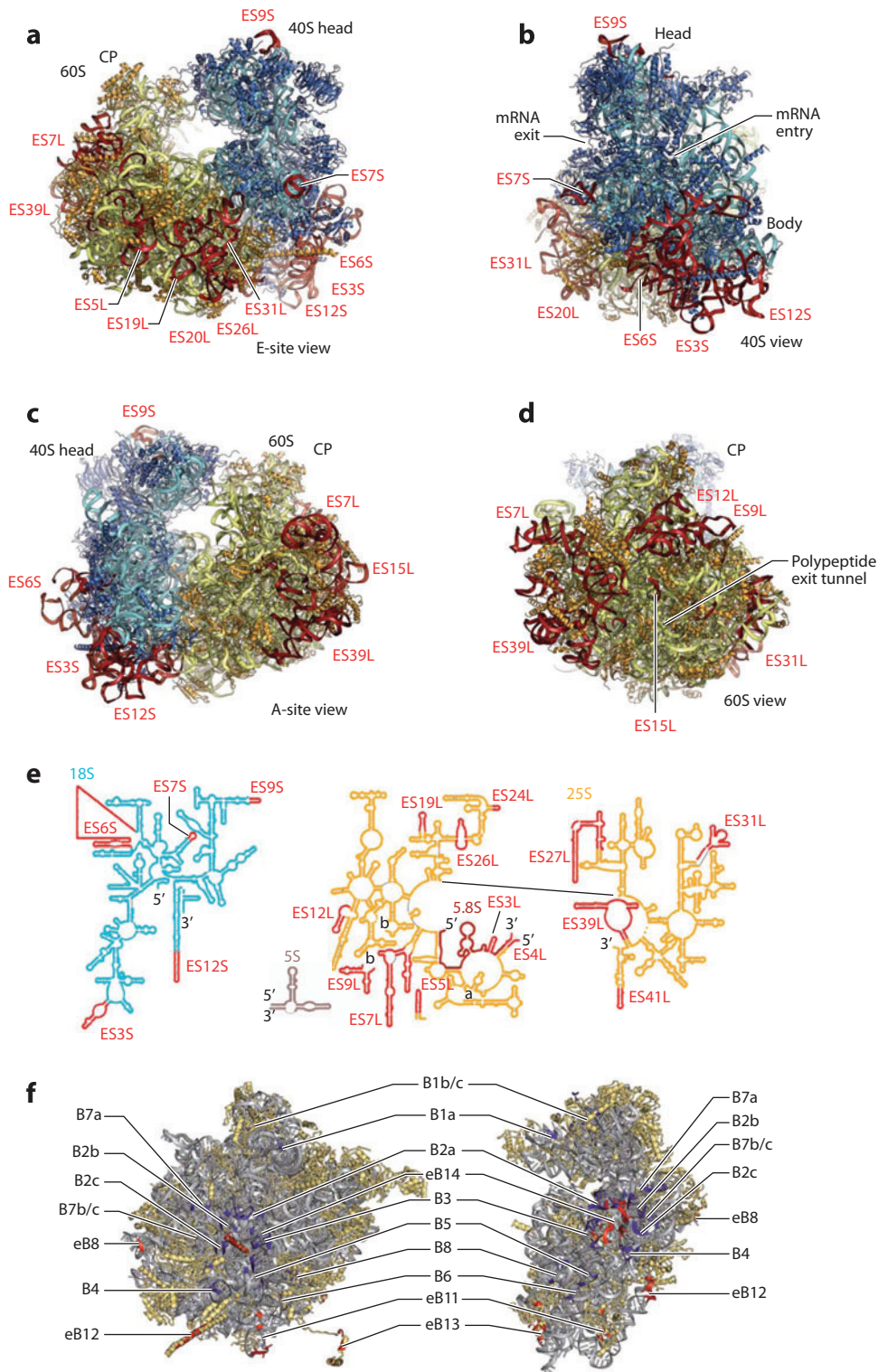


**Figure 4**

Crystal structure of the *Saccharomyces cerevisiae* 80S ribosome. Views from (a) the E site, (b) the small subunit side, (c) the A site, and (d) the large subunit side. The large subunit is shown in yellow with orange proteins, and the small subunit is shown in cyan with blue proteins. Eukaryote expansion segments (ESs) are shown in red.

(e) Secondary structure of yeast ribosomal RNA with E-site expansion segments (ESs) marked. (f) Interface view, showing residues forming eukaryote-specific bridges in red and conserved ones in blue. Protein L19e is involved in forming bridge eB12. Protein L24e extends from the 60S body to interact with S6e on the small subunit to form bridge eB13. Protein L41e forms bridge eB14. Abbreviations: CP, central protuberance; mRNA, messenger RNA.

protein L41e forms only minor contacts with the 60S subunit, it remains part of the large subunit upon dissociation. In bacteria, there is only one example of such an unusual bridge; it is formed by a ribosomal protein of the large subunit and binds to the small subunit through substantial parts of their structures (62). This unusual bridge is formed by protein L31, which is conserved among bacteria, and connects the central protuberance of the large subunit with the labile head domain of the small subunit.

The distinguishing features of the eukaryotic large subunit are two long protein helices, extending from the left and right sides, that are markedly distinct from the bridges of the core. These helices, which are eukaryote-specific additions to proteins L19e and L24e, create two bridges, eB12 and eB13, respectively, that are not buried within the intersubunit interface and are accessible from the solvent side. Bridge eB12, appearing below the mRNA exit tunnel, is formed mainly through multiple interactions between several turns of the 60-residue-long  $\alpha$ -helical extension at the C terminus of protein L19e and ES6S (Figures 2b, 4f). Protein L24e consists of an N-terminal domain that resides in the 60S subunit as well as a long, flexible linker that protrudes deep into the side of the 40S subunit body and a C-terminal domain that reaches the back of the 40S subunit. One should keep the architecture of protein L24e in mind, given the finding that protein L24e is crucial to the translation reinitiation of polycistronic mRNAs (63–65).

### Peptide Exit Tunnel

During translation, the growing peptide chain passes through the peptide exit tunnel to emerge at the solvent side, where it undergoes processing and folding. Recent X-ray structures and cryo-EM reconstructions of bacterial, archaeal, and eukaryotic ribosomes have shown that the dimensions of these exit tunnels are almost identical. The 100-Å-long, 10- to 20-Å-wide, irregularly shaped tunnel spans the entire body of the subunit. Increasing evidence indicates that the tunnel is a functionally important compartment in which the structure of the

nascent peptide is monitored and from which specific peptides can signal the ribosome to decrease its rate of elongation or even completely stop translation (66–69).

In bacteria and archaea, the tunnel walls are formed mainly by the conserved portions of the 23S rRNA and contain loops of proteins L4 and L22 and a bacteria-specific extension of L23 (Figure 5a) (11, 40, 43, 59, 70). In eukaryotes, the area corresponding to the bacteria-specific moieties of protein L23 overlaps with protein L39e (Figure 5b) (31, 34). In both the 50S and the 60S subunits, proteins L4 and L22 form a constriction of the tunnel that is located  $\sim 30$  Å from the peptidyl transferase center. In eukaryotes, the constriction is narrower because of insertions in protein L4. Although the role of these differences between bacteria and eukaryotes is unclear, the narrower size of the constriction in eukaryotes may block the access of some macrolide antibiotics to the peptidyl transferase center (71, 72). Investigators have suggested that these antibiotics must be delivered to the binding site through the tunnel. Genetic studies have revealed that insertion of six amino acids into the loop of protein L4 in *Escherichia coli* endows bacterial ribosomes with resistance to large macrolides, similar to what is found in eukaryotes.

On the solvent side, the rim of the polypeptide exit tunnel contains several bacteria- or eukaryote-specific proteins and protein extensions: proteins L17, L22, and an insertion in protein L24 in bacteria and proteins L39e and L31e in eukaryotes (Figure 5c,d). These differences are partly associated with the different processing of the N termini of nascent chains in bacteria versus eukaryotes.

## PERSPECTIVES OF YEAST RIBOSOME CRYSTALLOGRAPHY

### Nonribosomal Protein Stm1

The stress-related protein Stm1 can associate with 80S ribosomes and inhibit translation, but the nature and role of these interactions are unknown (73, 74). In the crystal structure of the vacant 80S ribosome, we found that Stm1

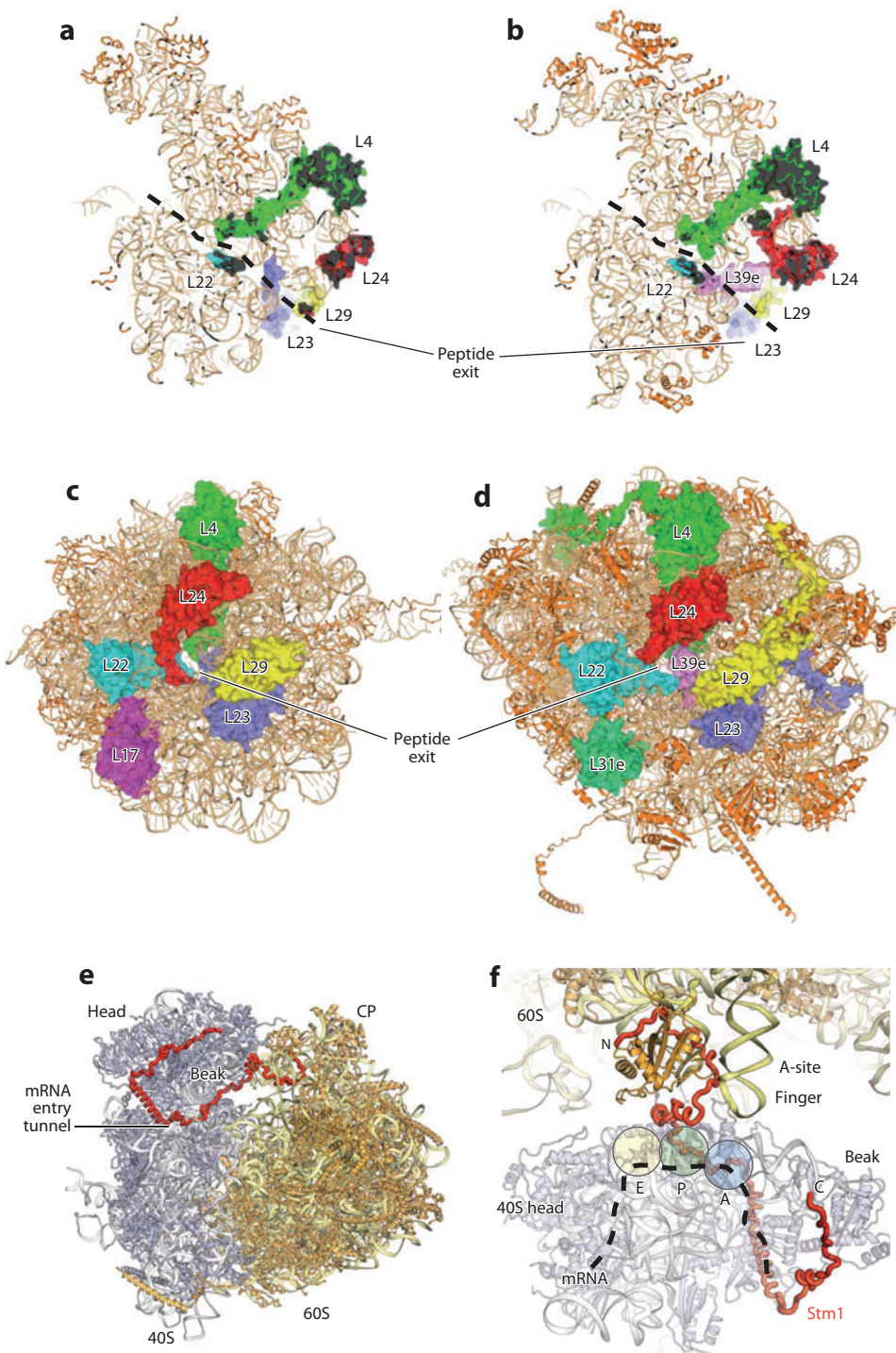


**Figure 5**

Crystal structure of the *Saccharomyces cerevisiae* 80S ribosome.

(a,b) Peptide exit tunnel indicated on the slice of the large subunits of (a) prokaryotes and (b) eukaryotes.

Ribosomal proteins involved in the tunnel structure are colored. (c,d) Structure of the peptide tunnel exit on the solvent side of the large ribosomal subunits of (c) 50S and (d) 60S. (e) Stm1 (red)

binds to the ribosomes 40S (blue) and 60S (yellow). (f) Top view of the 40S head and the 60S central protuberance (CP),

showing how Stm1 follows the messenger RNA (mRNA) pathway to the P site. The dashed black line

represents the path of the mRNA according to crystal structures of bacterial ribosomes (48, 49). The

approximate locations of the A, P, and E transfer RNA sites are indicated.

binds to the head domain of 40S and prevents mRNA access by inserting an  $\alpha$ -helix through the mRNA entry tunnel (**Figure 5e,f**). Furthermore, Stm1 is bound inside the mRNA tunnel from the mRNA entry tunnel through the P site, where it effectively blocks binding of tRNA and mRNA at the A and P sites, thereby preventing the formation of any functional ribosome complexes (**Figure 5f**) (31). The protein then crosses to the 60S subunit between the 5S rRNA and protein L5. By interacting with the ribosome in this way, Stm1 prevents subunit dissociation and stabilizes the 80S particle.

For preparation of functional ribosome complexes containing mRNA and tRNA ligands, the investigator's first challenge is to remove Stm1 from the ribosome. One can do so either by elaborating on the existing isolation procedure for Stm1-containing 80S ribosomes or by deleting it from the yeast genome, which is not lethal (75).

### Translocation and Domain Motions

The 80S crystal structure consists of two ribosome molecules in the asymmetric unit termed

ribosomes A and B. As described above, they differ markedly in terms of the degree of rotation of the 40S subunit relative to the 60S subunit ( $4^\circ$  for ribosome A and  $9^\circ$  for ribosome B) and the extent of 40S subunit head swiveling ( $15.5^\circ$  for ribosome A and  $10.5^\circ$  for ribosome B) relative to the unrotated 70S state (49). Previous cryo-EM and crystallographic studies (76–79) demonstrated that the two subunits rotate and swivel relative to one another during protein synthesis to allow for the translocation of tRNA and mRNA along the subunit interface. The two conformations that are observed in the 80S crystal structures appear to be related to the two states that occur prior to (molecule A) and immediately after (molecule B) translocation of tRNA and mRNA across the interface of the ribosome, as deduced from recent cryo-EM and crystallographic studies of the ribosome in different states (28, 80). The crystal structure of the 80S *S. cerevisiae* ribosome provides a unique opportunity for further studies of translocation events involved in the conformational changes that occur during translation.

#### SUMMARY POINTS

1. The first crystal structure of the eukaryotic ribosome has been determined.
2. Eukaryote-specific elements of rRNA and ribosomal proteins have been interpreted and localized on the solvent side of the ribosome structure.
3. The conservative organization of the ribosomal interface and ribosomal functional sites has been confirmed.
4. Yeast ribosome crystals have two ribosome conformations in one asymmetric unit. These conformations correspond to the functional states of the ribosome in translocation.
5. The nonribosomal protein Stm1 has been found in the empty ribosome structure.
6. New nomenclature for eukaryotic ribosomal proteins, based on bacterial ribosome structure and nomenclature, has been proposed.

#### FUTURE ISSUES

1. To study mechanisms of regulation of translation in eukaryotes, investigators should undertake the formation and crystallization of ribosome functional complexes.

2. Knowledge about yeast ribosome crystallography can be exploited for crystallization and structure determination of the human ribosome.
3. Investigators should study yeast ribosome structure with eukaryote-specific antibiotics.

## DISCLOSURE STATEMENT

The authors are not aware of any affiliations, memberships, funding, or financial holdings that might be perceived as affecting the objectivity of this review.

## ACKNOWLEDGMENTS

We thank Drs. Adam Ben-Shem, Sergey Melnikov, Nicolas Garreau de Loubresse, Lasse Jenner, and all of the other members of our laboratory. We are grateful to Dr. Sergey Melnikov for their help in preparation of **Figure 5** and for providing the video of overall views of prokaryotic and eukaryotic ribosomes. Our work was supported by a European Molecular Biology Organization long-term fellowship, the Human Frontier Science Program, and grants from the French National Research Agency (ANR BLAN07-3-190451 and ANR-07-PCVI-0015-01).

## LITERATURE CITED

1. Melnikov S, Ben-Shem A, Garreau de Loubresse N, Jenner L, Yusupova G, Yusupov M. 2012. One core, two shells: bacterial and eukaryotic ribosomes. *Nat. Struct. Mol. Biol.* 19:560–67
2. Frank J, Verschoor A, Li Y, Zhu J, Lata RK, et al. 1995. A model of the translational apparatus based on a three-dimensional reconstruction of the *Escherichia coli* ribosome. *Biochem. Cell Biol.* 73:757–65
3. Stark H, Orlova EV, Rinke-Appel J, Jünke N, Mueller F, et al. 1997. Arrangement of tRNAs in pre- and posttranslocational ribosomes revealed by electron cryomicroscopy. *Cell* 88:19–28
4. Stark H, Rodnina MV, Rinke-Appel J, Brimacombe R, Wintermeyer W, van Heel M. 1997. Visualization of elongation factor Tu on the *Escherichia coli* ribosome. *Nature* 389:403–6
5. Agrawal RK, Penczek P, Grassucci RA, Frank J. 1998. Visualization of elongation factor G on the *Escherichia coli* 70S ribosome: the mechanism of translocation. *Proc. Natl. Acad. Sci. USA* 95:6134–18
6. Cate JH, Yusupov M, Yusupova G, Earnest TN, Noller HF. 1999. X-ray crystal structures of 70S ribosome functional complexes. *Science* 285:2095–104
7. Clemons WM Jr, May JL, Wimberly BT, McCutcheon JP, Capel MS, Ramakrishnan V. 1999. Structure of a bacterial 30S ribosomal subunit at 5.5 Å resolution. *Nature* 400:833–40
8. Ban N, Freeborn B, Nissen P, Penczek P, Grassucci RA, et al. 1998. A 9 Å resolution X-ray crystallographic map of the large ribosomal subunit. *Cell* 93:1105–15
9. Ban N, Nissen P, Hansen J, Capel M, Moore PB, Steitz TA. 1999. Placement of protein and RNA structures into a 5 Å resolution map of the 50S ribosomal subunit. *Nature* 400:841–47
10. Wimberly BT, Brodersen DE, Clemons WM Jr, Morgan-Warren RJ, Carter AP, et al. 2000. Structure of the 30S ribosomal subunit. *Nature* 407:327–39
11. Ban N, Nissen P, Hansen J, Moore PB, Steitz TA. 2000. The complete atomic structure of the large ribosomal subunit at 2.4 Å resolution. *Science* 289:905–20
12. Yusupov M, Yusupova G, Baucom A, Lieberman K, Earnest TN, et al. 2001. Crystal structure of the ribosome at 5.5 Å resolution. *Science* 292:883–96
13. Yonath A, Müssig J, Wittmann HG. 1982. Parameters for crystal growth of ribosomal subunits. *J. Cell. Biochem.* 19:145–55
14. Yonath A, Piefke J, Müssig J, Gewitz HS, Wittmann HG. 1983. A compact three-dimensional crystal form of the large ribosomal subunit from *Bacillus stearothermophilus*. *FEBS Lett.* 163:69–72

15. Harel M, Shoham M, Frolow F, Eisenberg H, Mevarech M, et al. 1988. Crystallization of halophilic malate dehydrogenase from *Halobacterium marismortui*. *J. Mol. Biol.* 200:609–10
16. Yusupov M, Barinin VV, Borovyagin BD, Garber M, Sedelnikova S, et al. 1987. Crystallization of the 30S subunits of *Thermus thermophilus* ribosomes. *Dokl. Akad. Nauk SSSR* 292:1271–74
17. Trakhanov SD, Yusupov M, Agalarov S, Garber M, Ryazantzev S, et al. 1987. Crystallization of 70S ribosomes and 30S ribosomal subunits from *Thermus thermophilus*. *FEBS Lett.* 220:319–22
18. Yusupova G, Yusupov M, Spirin A, Ebel JP, Moras D, et al. 1991. Formation and crystallization of *Thermus thermophilus* 70S ribosome/tRNA complexes. *FEBS Lett.* 290:69–72
19. Trakhanov S, Yusupov M, Shirokov V, Garber M, Mitschler A, et al. 1989. Preliminary X-ray investigation of 70 S ribosome crystals from *Thermus thermophilus*. *J. Mol. Biol.* 209:327–28
20. Garber M, Agalarov C, Eliseikina I, Tischenko S, Shirokov V, et al. 1991. Purification and crystallization of components of the protein-synthesizing system from *Thermus thermophilus*. *J. Cryst. Growth* 110:228–36
21. Steitz TA. 2008. A structural understanding of the dynamic ribosome machine. *Nat. Rev. Mol. Cell Biol.* 9:242–53
22. Schmeing TM, Ramakrishnan V. 2009. What recent ribosome structures have revealed about the mechanism of translation. *Nature* 461:1234–42
23. Demeshkina N, Jenner L, Yusupova G, Yusupov M. 2010. Interactions of the ribosome with mRNA and tRNA. *Curr. Opin. Struct. Biol.* 20:325–32
24. Spahn CM, Beckmann R, Eswar N, Penczek PA, Sali A, et al. 2001. Structure of the 80S ribosome from *Saccharomyces cerevisiae*–tRNA–ribosome and subunit–subunit interactions. *Cell* 107:373–86
25. Spahn CM, Gomez-Lorenzo MG, Grassucci RA, Jørgensen R, Andersen GR, et al. 2004. Domain movements of elongation factor eEF2 and the eukaryotic 80S ribosome facilitate tRNA translocation. *EMBO J.* 23:1008–19
26. Becker T, Bhushan S, Jarasch A, Armache JP, Funes S, et al. 2009. Structure of monomeric yeast and mammalian Sec61 complexes interacting with the translating ribosome. *Science* 326:1369–73
27. Fu J, Munro JB, Blanchard SC, Frank J. 2011. Cryoelectron microscopy structures of the ribosome complex in intermediate states during tRNA translocation. *Proc. Natl. Acad. Sci. USA* 108:4817–21
28. Ratje AH, Loerke J, Mikolajka A, Brüner M, Hildebrand PW, et al. 2010. Head swivel on the ribosome facilitates translocation by means of intra-subunit tRNA hybrid sites. *Nature* 468:713–16
29. Fischer N, Konevega AL, Wintermeyer W, Rodnina MV, Stark H. 2010. Ribosome dynamics and tRNA movement by time-resolved electron cryomicroscopy. *Nature* 466:329–33
30. Seidelt B, Innis CA, Wilson DN, Gartmann M, Armache JP, et al. 2009. Structural insight into nascent polypeptide chain-mediated translational stalling. *Science* 326:1412–15
31. Ben-Shem A, Garreau de Loubresse N, Melnikov S, Jenner L, Yusupova G, Yusupov M. 2011. The structure of the eukaryotic ribosome at 3.0 Å resolution. *Science* 334:1524–29
32. Ben-Shem A, Jenner L, Yusupova G, Yusupov M. 2010. Crystal structure of the eukaryotic ribosome. *Science* 330:1203–9
33. Rabl J, Leibundgut M, Ataide SF, Haag A, Ban N. 2010. Crystal structure of the eukaryotic 40S ribosomal subunit in complex with initiation factor 1. *Science* 331:730–36
34. Klinge S, Voigts-Hoffmann F, Leibundgut M, Arpagaus S, Ban N. 2011. Crystal structure of the eukaryotic 60S ribosomal subunit in complex with initiation factor 6. *Science* 334:941–48
35. Rabl J, Leibundgut M, Ataide SF, Haag A, Ban N. 2011. Crystal structure of the eukaryotic 40S ribosomal subunit in complex with initiation factor 1. *Science* 331:730–36
36. Klaholz BP, Myasnikov AG, Van Heel M. 2004. Visualization of release factor 3 on the ribosome during termination of protein synthesis. *Nature* 427:862–65
37. Gogia ZV, Yusupov M, Spirina TN. 1986. Structure of *Thermus thermophilus* ribosomes. Method of isolation and purification of the ribosomes. *Mol. Biol.* 20:519–26
38. Fechter P, Chevalier C, Yusupova G, Yusupov M, Romby P, Marzi S. 2009. Ribosomal initiation complexes probed by toeprinting and effect of *trans*-acting translational regulators in bacteria. *Methods Mol. Biol.* 540:247–63

39. Clemons WM Jr, Brodersen DE, McCutcheon JP, May JL, Carter AP, et al. 2001. Crystal structure of the 30 S ribosomal subunit from *Thermus thermophilus*: purification, crystallization and structure determination. *J. Mol. Biol.* 310:827–43
40. Selmer M, Dunham CM, Murphy FV IV, Weixlbaumer A, Petry S, et al. 2006. Structure of the 70S ribosome complexed with mRNA and tRNA. *Science* 313:1935–42
41. Ben-Shem A, Frolov F, Nelson N. 2003. Crystal structure of plant photosystem I. *Nature* 426:630–35
42. Ashe MP, De Long SK, Sachs AB. 2000. Glucose depletion rapidly inhibits translation initiation in yeast. *Mol. Biol. Cell* 11:833–48
43. Jenner L, Demeshkina N, Yusupova G, Yusupov M. 2010. Structural aspects of messenger RNA reading frame maintenance by the ribosome. *Nat. Struct. Mol. Biol.* 17:555–60
44. Komili S, Farny NG, Roth FP, Silver PA. 2007. Functional specificity among ribosomal proteins regulates gene expression. *Cell* 131:557–71
45. Smith TF, Lee JC, Gutell RR, Hartman H. 2008. The origin and evolution of the ribosome. *Biol. Direct* 3:16
46. Lecompte O, Ripp R, Thierry JC, Moras D, Poch O. 2002. Comparative analysis of ribosomal proteins in complete genomes: an example of reductive evolution at the domain scale. *Nucleic Acids Res.* 30:5382–90
47. Gerbi SA. 1986. The evolution of eukaryotic ribosomal DNA. *Biosystems* 19:247–58
48. Yusupova G, Yusupov M, Cate JH, Noller HF. 2001. The path of messenger RNA through the ribosome. *Cell* 106:233–41
49. Jenner LB, Demeshkina N, Yusupova G, Yusupov M. 2010. Structural aspects of messenger RNA reading frame maintenance by the ribosome. *Nat. Struct. Mol. Biol.* 17:555–60
50. Carter AP, Clemons WM, Brodersen DE, Morgan-Warren RJ, Wimberly BT, Ramakrishnan V. 2000. Functional insights from the structure of the 30S ribosomal subunit and its interactions with antibiotics. *Nature* 407:340–48
51. Demeshkina N, Jenner L, Westhof E, Yusupov M, Yusupova G. 2012. A new understanding of the decoding principle on the ribosome. *Nature* 484:256–59
52. Simonovic M, Steitz TA. 2009. A structural view on the mechanism of the ribosome-catalyzed peptide bond formation. *Biochim. Biophys. Acta* 1789:612–23
53. Wilson DN, Doudna Cate JH. 2012. The structure and function of the eukaryotic ribosome. *Cold Spring Harb. Perspect. Biol.* 4:011536
54. Sonenberg N, Hinnebusch AG. 2009. Regulation of translation initiation in eukaryotes: mechanisms and biological targets. *Cell* 136:731–45
55. Jackson RJ, Hellen CU, Pestova TV. 2010. The mechanism of eukaryotic translation initiation and principles of its regulation. *Nat. Rev. Mol. Cell Biol.* 11:113–27
56. Mager WH, Planta RJ, Ballesta JG, Lee JC, Mizuta K, et al. 1997. A new nomenclature for the cytoplasmic ribosomal proteins of *Saccharomyces cerevisiae*. *Nucleic Acids Res.* 25:4872–75
57. Marintchev A, Edmonds KA, Marintcheva B, Hendrickson E, Oberer M, et al. 2009. Topology and regulation of the human eIF4A/4G/4H helicase complex in translation initiation. *Cell* 136:447–60
58. Pomeranz Krummel DA, Oubridge C, Leung AK, Li J, Nagai K. 2009. Crystal structure of human spliceosomal U1 snRNP at 5.5 Å resolution. *Nature* 458:475–80
59. Schuwirth BS, Borovinskaya MA, Hau CW, Zhang W, Vila-Sanjurjo A, et al. 2005. Structures of the bacterial ribosome at 3.5 Å resolution. *Science* 310:827–34
60. Spahn CM, Gomez-Lorenzo MG, Grassucci RA, Jørgensen R, Andersen GR, et al. 2004. Domain movements of elongation factor eEF2 and the eukaryotic 80S ribosome facilitate tRNA translocation. *EMBO J.* 23:1008–19
61. Budkevich T, Giesebrecht J, Altman RB, Munro JB, Mielke T, et al. 2011. Structure and dynamics of the mammalian ribosomal pretranslocation complex. *Mol. Cell* 44:214–24
62. Jenner L, Demeshkina N, Yusupova G, Yusupov M. 2010. Structural rearrangements of the ribosome at the tRNA proofreading step. *Nat. Struct. Mol. Biol.* 17:1072–78
63. Park HS, Himmelbach A, Browning KS, Hohn T, Ryabova LA. 2001. A plant viral “reinitiation” factor interacts with the host translational machinery. *Cell* 106:723–33
64. Nishimura T, Wada T, Yamamoto KT, Okada K. 2005. The *Arabidopsis* STV1 protein, responsible for translation reinitiation, is required for auxin-mediated gynoecium patterning. *Plant Cell* 17:2940–53

65. Thiebauld O, Schepetilnikov M, Park HS, Geldreich A, Kobayashi K, et al. 2009. A new plant protein interacts with eIF3 and 60S to enhance virus-activated translation re-initiation. *EMBO J.* 28:3171–84
66. Vázquez-Laslop N, Mankin AS. 2011. Picky nascent peptides do not talk to foreign ribosomes. *Proc. Natl. Acad. Sci. USA* 108:5931–32
67. Wilson DN, Beckmann R. 2011. The ribosomal tunnel as a functional environment for nascent polypeptide folding and translational stalling. *Curr. Opin. Struct. Biol.* 21:274–82
68. Cruz-Vera LR, Sachs MS, Squires CL, Yanofsky C. 2011. Nascent polypeptide sequences that influence ribosome function. *Curr. Opin. Microbiol.* 14:160–66
69. Tenson T, Ehrenberg M. 2002. Regulatory nascent peptides in the ribosomal tunnel. *Cell* 108:591–94
70. Harms J, Schlutzen F, Zarivach R, Bashan A, Gat S, et al. 2001. High resolution structure of the large ribosomal subunit from a mesophilic eubacterium. *Cell* 107:679–88
71. Tu D, Blaha G, Moore PB, Steitz TA. 2005. Structures of MLSBK antibiotics bound to mutated large ribosomal subunits provide a structural explanation for resistance. *Cell* 121:257–70
72. Zaman S, Fitzpatrick M, Lindahl L, Zengel J. 2007. Novel mutations in ribosomal proteins L4 and L22 that confer erythromycin resistance in *Escherichia coli*. *Mol. Microbiol.* 66:1039–50
73. Van Dyke N, Baby J, Van Dyke MW. 2006. Stm1p, a ribosome-associated protein, is important for protein synthesis in *Saccharomyces cerevisiae* under nutritional stress conditions. *J. Mol. Biol.* 358:1023–31
74. Balagopal V, Parker R. 2011. Stm1 modulates translation after 80S formation in *Saccharomyces cerevisiae*. *RNA* 17:835–42
75. Ligr M, Velten I, Fröhlich E, Madeo F, Ledig M, et al. 2001. The proteasomal substrate Stm1 participates in apoptosis-like cell death in yeast. *Mol. Biol. Cell* 12:2422–32
76. Frank J, Agrawal RK. 2000. A ratchet-like inter-subunit reorganization of the ribosome during translocation. *Nature* 406:318–22
77. Horan LH, Noller HF. 2007. Intersubunit movement is required for ribosomal translocation. *Proc. Natl. Acad. Sci. USA* 104:4881–85
78. Zhang W, Dunkle JA, Cate JH. 2009. Structures of the ribosome in intermediate states of ratcheting. *Science* 325:1014–17
79. Zhou J, Lancaster L, Trakhanov S, Noller HF. 2012. Crystal structure of release factor RF3 trapped in the GTP state on a rotated conformation of the ribosome. *RNA* 18:230–40
80. Dunkle JA, Wang L, Feldman MB, Pulk A, Chen VB, et al. 2011. Structures of the bacterial ribosome in classical and hybrid states of tRNA binding. *Science* 332:981–84
81. Halic M, Becker T, Frank J, Spahn CM, Beckmann R. 2005. Localization and dynamic behavior of ribosomal protein L30e. *Nat. Struct. Mol. Biol.* 12:467–68
82. Chandramouli P, Topf M, Menetret JF, Eswar N, Cannone JJ, et al. 2008. Structure of the mammalian 80S ribosome at 8.7 Å resolution. *Structure* 16:535–48
83. Strunk BS, Karbstein K. 2009. Powering through ribosome assembly. *RNA* 15:2083–104
84. Wilson DN, Beckmann R. 2011. The ribosomal tunnel as a functional environment for nascent polypeptide folding and translational stalling. *Curr. Opin. Struct. Biol.* 21:274–82
85. Brandt F, Carlson LA, Hartl FU, Baumeister W, Grünewald K. 2010. The three-dimensional organization of polyribosomes in intact human cells. *Mol. Cell* 39:560–69
86. Wilson DN, Beckmann R. 2011. The ribosomal tunnel as a functional environment for nascent polypeptide folding and translational stalling. *Curr. Opin. Struct. Biol.* 21:274–82
87. Brandt F, Etchells SA, Ortiz JO, Elcock AH, Hartl FU, Baumeister W. 2009. The native 3D organization of bacterial polysomes. *Cell* 136:261–71